

CHAPTER 5

MEASURING THE TENSOR TRANSITION POLARIZABILITY

As discussed in Chapter 1, the standard model can be tested by extracting the value of the weak charge Q_W from the equation

$$\frac{\text{Im}(E_{\text{PNC}})}{\beta} = -i \frac{Q_W}{\beta N} k_{\text{PNC}}, \quad (5.1)$$

where the value of $\text{Im}(E_{\text{PNC}})/\beta$ has been measured to 0.35% [13]. Also discussed was the fact that atomic theory calculations are needed to determine the values of k_{PNC} and β^* . Because the uncertainty in the theory is the limiting factor in the test of the standard model, it is desirable to reduce the dependence on theory by making an independent measurement of β .

While the measurements of the dc Stark shift and β are both accomplished by scanning a dye laser across the $6S \rightarrow 7S$ transition and measuring the transition rate as a function of frequency, the latter experiment is susceptible to many more problems. Measuring the dc Stark shift requires only the accurate measurement of the frequency separation of two spectral lines. The line shapes, contributions from background signals, magnetic field perturbations, and contamination of the signal from unwanted amplitudes are all examples of effects that do not affect the dc Stark shift measurement but are important for measuring β .

This chapter details our measurement of β . It begins with a description

* β has also been determined semi-empirically, but the calculation from the atomic theory has higher precision.

of the basic idea behind the measurement and continues with a detailed discussion of the experimental complications that must be addressed to make an accurate and precise measurement. The raw data are then presented, and the chapter concludes by covering the issue of the presence of an electric quadrupole transition. The electric quadrupole amplitude has affected previous experiments, and its effects must be considered carefully in the present measurement. A full mathematical treatment of these effects is given in Appendix B.

5.1 Experimental Concept

As discussed in Section 2.7, in order to determine β , we need to first measure the $E1$ and $M1$ amplitudes on the $\Delta F = \pm 1$ transitions. We do this by scanning the dye laser across the appropriate $6S \rightarrow 7S$ transitions and integrating the total fluorescence collected on the probe photodiode. These integrated areas are proportional to the transition rates. If we then take the ratio of the $M1$ area (measured with no applied E) and the $E1$ area (measured with $E = 700$ V/cm), all the unknown parameters (such as beam flux, probe detection efficiency, and intensity inside the PBC) cancel, and to a good approximation we are left with the ratios

$$R^\pm \equiv \left(\frac{M \mp M_{\text{hf}}}{\beta E} \right)^2, \quad (5.2)$$

where R^\pm correspond to the $\Delta F = \pm 1$ transitions. From these ratios we can extract the value of M_{hf}/β . [See Eq. (5.6) and Eq. (5.7) for minor corrections.] Then we can use the value of M_{hf} determined in Ref. [27] to extract β . The amplitude M_{hf} can be determined very precisely because it is related to the well-known hyperfine splittings of cesium. The goal is to measure M_{hf}/β with a precision of 0.1%. The uncertainty in the final value of β is then dominated by the 0.25% determination of M_{hf} [27].

quantity we want to measure is given by

$$A_{\text{Total}} = \int_{-\infty}^{\infty} h(\nu) d\nu. \quad (5.3)$$

Of course, we make measurements of the signal size at discrete frequencies, and we can only scan the frequency of the laser within its tunable frequency range. In addition, we cannot measure $h(\nu)$ directly. Rather, we must calculate it from the difference between $f(\nu)$ and $BG(\nu)$. We then have

$$\begin{aligned} A_{\text{Total}} &= \sum_{i=-\infty}^{\infty} [f(\nu_i) - BG(\nu_i)] \Delta\nu_i \\ &= \sum_{i < a} [f(\nu_i) - BG(\nu_i)] \Delta\nu_i + \sum_{i=a}^b [f(\nu_i) - BG(\nu_i)] \Delta\nu_i \\ &\quad + \sum_{i > b} [f(\nu_i) - BG(\nu_i)] \Delta\nu_i \\ &= A_{\text{low}} + A_{\text{measured}} + A_{\text{high}}. \end{aligned} \quad (5.4)$$

Clearly we must choose a and b such that A_{low} and A_{high} are negligible. Then we are left with A_{measured} . We are still left with two problems: the noise on the background and the fact that we can only measure $f(\nu_i)$, not $h(\nu_i)$ and $BG(\nu_i)$.

If the background is a linear function of frequency then we can measure its value at a low reference point and a high reference point where the contribution from $h(\nu_i)$ is negligible. Then, if these two reference points are centered around the peak of the transition, we can take their average and use $\sum [f(\nu_i) - BG(\nu_i)] = \sum [f(\nu_i) - BG_{\text{AVG}}]$ to subtract off the contribution from the background. If the background is nonlinear, this method does not give the right answer.

The contributions to the background level from known sources are all essentially linear functions of the dye laser frequency or independent of it. These sources are atoms left in the wrong hyperfine state, scattered light from the PBC mirrors, and scattered light from the probe and hyperfine pumping lasers. The only contri-

bution to the background that might be nonlinear is from molecules interacting with the dye laser and being detected by the probe laser in a frequency sensitive manner. However, we measure the background with varying oven nozzle temperatures (which vary the fraction of Cs_2 molecules in the beam) and find no measurable molecular background. Therefore, the procedure in the previous paragraph does give the correct answer.

Another complication is the fact that there is noise on the background, and this $1/f$ noise is our limiting source of noise. Thus, if we measure the background at the high and low reference points and subsequently scan across the transition, the background will be slightly different at each measurement of $f(\nu_i)$ than it was when we first measured it. To solve this problem, we take advantage of our ~ 25 Hz data taking frequency: before and after **each** measurement of $f(\nu_i)$ we measure the background at the high and low reference points. In this way we get the average background **at the time of the measurement** of $f(\nu_i)$. We also alternate which reference comes first to eliminate problems that might arise due to hysteresis.

Finally, we must know the frequency separation $\Delta\nu_i$ between each measurement of the transition rate. This is because we are essentially determining the area of the line shape using the trapezoidal rule. We must know both the height and the width of each “rectangle” we use to determine the total area. If the rectangles are not of uniform width and we assume they are, we will get an incorrect result. Therefore, we calibrate the control voltage from the computer to obtain sufficient accuracy in our knowledge of ν_i .

5.2.2 Comparing the Areas Correctly

As mentioned in Chapter 4, the line shapes of the $6S \rightarrow 7S$ transition are asymmetric because of the ac Stark effect [30]. The ac Stark effect causes another problem: it shifts and distorts the $M1$ transitions differently from the $E1$ transitions. This is because the $E1$ transition is driven by the oscillating electric field (ϵ_{ac}) of

the laser and the $M1$ transitions are driven by the oscillating magnetic field (b_{ac}) of the laser, while the ac Stark effect causes the largest shift where ϵ_{ac} is large. Thus, in the regions of large ϵ_{ac} there is a large ac Stark shift and a high* probability of driving an $E1$ transition. In regions of small ϵ_{ac} (and a correspondingly large b_{ac}) there is a small ac Stark shift and a large probability of driving an $M1$ transition. This effect is shown dramatically in Fig. 5.2.

If the line shapes for the two transitions had simple Voigt profiles with the same widths, for example, and we missed 1% of each area in the wings, the ratio will still be correct. That is $M1/\beta = (0.99 \times M1)/(0.99 \times \beta)$. However, since the two line shapes do not have the same width and they are offset, it would be easy to miss 1% of β and only miss 0.1% of $M1$. We avoid this problem by making the scans across the transitions wide enough to measure all the area for both transitions. We also confirm that the scan width is wide enough by reanalyzing the data by omitting increasingly large amounts of data from the beginning and end of the scans. We do not find a significant variation in the ratios when we do the reanalysis.

The discussion so far has implied that all we need to do is scan across the $M1$ transition and then scan across the $E1$ transition and we have the two values we need to determine the ratio. However, when we scan across the $E1$ transition, the $M1$ transition is not absent, it is just very small. The ratio we actually measure is

$$R_{\text{measured}}^{\pm} = \frac{(M \mp M_{\text{hf}})^2}{\beta^2 E^2 + (M \mp M_{\text{hf}})^2}. \quad (5.5)$$

The ratio we actually want is given by

$$R^{\pm} = \frac{(M \mp M_{\text{hf}})^2}{\beta^2 E^2} = \frac{R_{\text{measured}}^{\pm}}{1 - R_{\text{measured}}^{\pm}}. \quad (5.6)$$

*The terms “high” and “low” are only used in the relative sense. For example, there may be a “high” probability of making a Stark-induced $E1$ transition, but that transition amplitude is over seven orders of magnitude smaller than the $D1$ electric dipole transition.

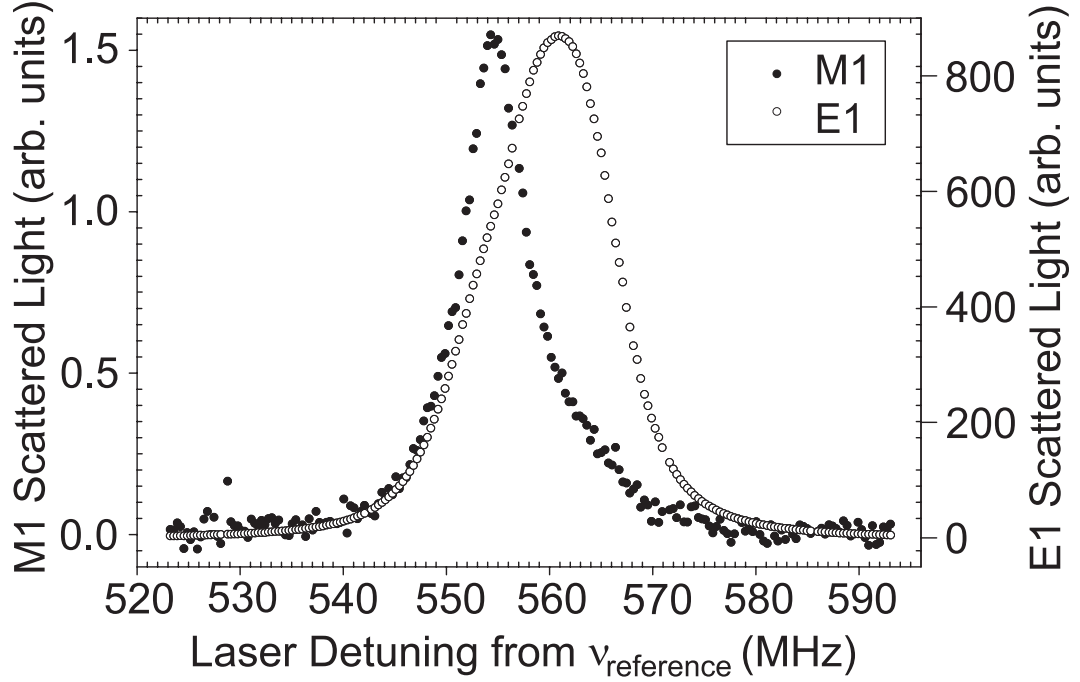


Figure 5.2: Plot comparing the $E1$ and $M1$ line shapes. The asymmetries in the line shapes and the differences in widths and center frequencies are due to the ac Stark effect as discussed in Ref. [30].

5.2.3 Photoionization Correction

Just as the ac Stark effect's dependence on ϵ_{ac} combines with the dependence of $E1$ on ϵ_{ac} and $M1$ on b_{ac} to give different line shapes, photoionization also causes a difference in detection efficiency between $E1$ and $M1$ because it is also maximum where ϵ_{ac} is maximum. This is explained in the following manner.

Atoms that are in a region with a large ϵ_{ac} have a high probability of making an $E1$ transition. The same atoms also have a high probability of being photoionized. Atoms in a region with a large b_{ac} have a high probability of making an $M1$ transition. However, these atoms have a small probability of being photoionized. Any atoms that are photoionized are no longer available to be detected downstream in the detection region. Thus, a smaller fraction of atoms that made the $E1$ transition is available for detection relative to the fraction of atoms that made the $M1$ transition.

The result is that as the intensity inside the PBC gets higher, the ratio $M \pm M_{\text{hf}}/\beta$ gets correspondingly larger. With this effect, the ratios on the two transitions are given by

$$R_I^\pm \equiv \left(\frac{M \mp M_{\text{hf}}}{\beta E} \right) (1 + \eta I). \quad (5.7)$$

The intensity inside the PBC is proportional to the power that is transmitted through the output mirror, which we measure on a photodiode. I is this voltage, and η is a parameter that describes the difference in photoionization probabilities. In order to correct for this effect, we must take data at several intensities and extrapolate the result to zero intensity. The data taken for this correction are shown in Section 5.3.

5.2.4 Non- B_z Magnetic Field Systematic Error

As mentioned in Section 2.6, a misaligned magnetic field can change the definition of the operator $\vec{\sigma}$. This, in turn, changes the rates we measure. Using Eq. (2.28) and Eq. (2.25) we find that the ratios we measure become

$$R = \frac{(M \mp M_{\text{hf}})^2 \sum_{m'_F} \left[\left(\frac{B_z}{B} \right)^2 (C_{Fm_F}^{F\pm 1m'_F})^2 \delta_{m'_F m_F \pm 1} + \left(\frac{B_x}{B} \right)^2 (C_{Fm_F}^{F\pm 1m'_F})^2 \delta_{m'_F m_F} \right]}{\beta^2 E^2 \sum_{m'_F} (C_{Fm_F}^{F\pm 1m'_F})^2} \quad (5.8)$$

for a small rotation of \vec{B} into the \hat{x} axis, and

$$R = \frac{(M \mp M_{\text{hf}})^2 \sum_{m'_F} (C_{Fm_F}^{F\pm 1m'_F})^2}{\beta^2 E^2 \sum_{m'_F} \left[\left(\frac{B_z}{B} \right)^2 (C_{Fm_F}^{F\pm 1m'_F})^2 \delta_{m'_F m_F \pm 1} + \left(\frac{B_y}{B} \right)^2 (C_{Fm_F}^{F\pm 1m'_F})^2 \delta_{m'_F m_F} \right]} \quad (5.9)$$

for a small rotation of \vec{B} into the \hat{y} axis. This would not be a problem if the populations of the m_F sublevels were uniform. This is because

$$\sum_{m_F} (C_{Fm_F}^{F\pm 1m_F})^2 = 2 \sum_{m_F} (C_{Fm_F}^{F\pm 1m_F \pm 1})^2. \quad (5.10)$$

Therefore, the ratios are constant, regardless of the value of B_x or B_y .

However, we know that pumping the atoms into a single hyperfine state redistributes the atoms in a nonuniform way. The populations from a uniform distribution, from a simple Monte Carlo rate equation simulation, and from a full quantum mechanical treatment are shown in Table 5.1. When we pump atoms into the $F = 3$ state, more atoms tend to fall into the Zeeman sublevels near $m_F = 0$, and when we pump atoms into the $F = 4$ state, more atoms tend to fall into the Zeeman sublevels near $|m_F| = 4$.

The $C_{Fm_F}^{F'm'_F}$ coefficients have a nonuniform dependence on the initial m_F state that is similar to the dependence of the Zeeman sublevel population distribution. The $\Delta m_F = 0$ transitions are stronger for transitions starting from near $m_F = 0$, and the $\Delta m_F = \pm 1$ transitions are weaker for the same transitions. The result is that on the $F = 3$ to $F' = 4$ ($F = 4$ to $F' = 3$) transitions the numerator gets larger (smaller) as \vec{B} rotates into \hat{x} and weights the $\Delta m_F = 0$ transitions more heavily. Similarly the denominator gets larger (smaller) as \vec{B} rotates into \hat{y} . This behavior has been verified experimentally. The results of the theory are compared

Table 5.1: The fractional population in a given Zeeman sublevel after hyperfine pumping has been performed. The uniform distribution assumes that no redistribution of the populations takes place. ‘‘Bennett’’ refers to the populations found using a simple Monte Carlo simulation of hyperfine pumping. ‘‘Marte’’ refers to the results of a full quantum mechanical calculation performed by Peter Marte [56].

F	m_F	Method			F	m_F	Method		
		Uniform	Bennett	Marte			Uniform	Bennett	Marte
3	3	0.1429	0.1030	0.1163	4	4	0.1111	0.1430	0.1230
	2	0.1429	0.1570	0.1442		3	0.1111	0.1308	0.1061
	1	0.1429	0.1598	0.1632		2	0.1111	0.1067	0.1038
	0	0.1429	0.1598	0.1666		1	0.1111	0.0831	0.1040
	-1	0.1429	0.1598	0.1593		0	0.1111	0.0749	0.1109
	-2	0.1429	0.1570	0.1369		-1	0.1111	0.0831	0.1028
	-3	0.1429	0.1030	0.1134		-2	0.1111	0.1067	0.1068
					-3	0.1111	0.1308	0.1104	
					-4	0.1111	0.1430	0.1321	

with data in Fig. 5.3. The results shown are for the $F = 4$ to $F' = 3$ transition with the magnetic field rotated into the \hat{x} direction. It is clear that the full quantum mechanical treatment gives reasonable qualitative agreement.

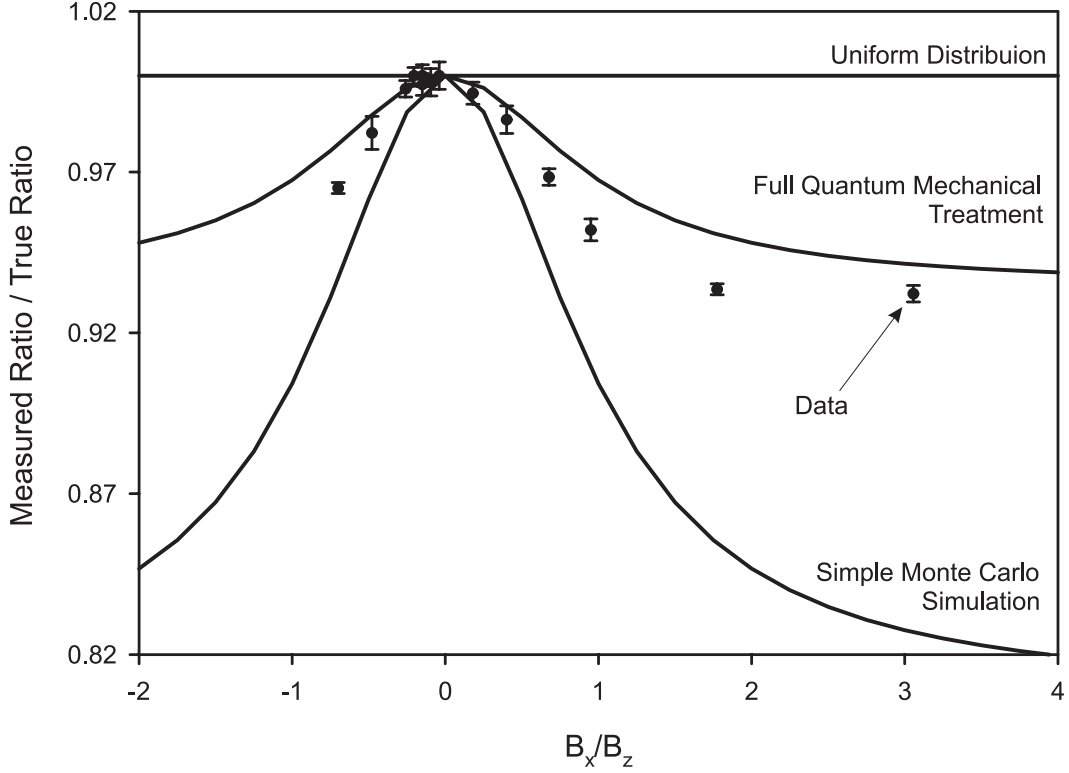


Figure 5.3: Data and theory showing the effect of misaligned \vec{B} on the ratio $M + M_{\text{hf}}/\beta$ on the $F = 4$ to $F' = 3$ transition. Here the magnetic field is rotated into the \hat{x} direction.

This error due to misaligned magnetic fields is the most serious systematic error we need to address. Using the data we collected (not the theoretical prediction), we find that in order to have the effect of a misaligned magnetic field contribute less than 0.02% we must keep B_x and B_y less than 220 mG when the main field is set at $B_z = 4$ G. This is an easy requirement to meet since we routinely kept these fields less than 1 mG for the PNC measurement. To confirm the absence of any effect we also take data with main magnetic fields smaller than 4 G. If there is a residual misaligned component, the fractional error in the ratio will get larger as the main

field gets smaller. These data are shown in Fig. 5.4. The fractional difference between

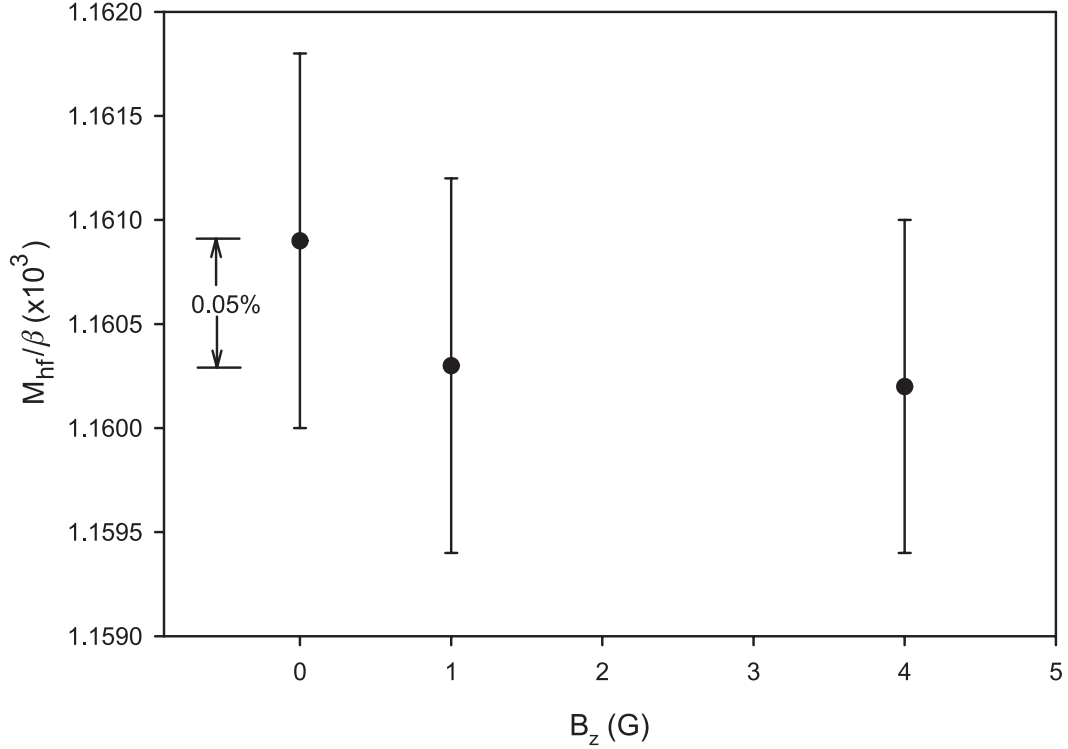


Figure 5.4: Measured ratios M_{hf}/β as a function of B_z . Any deviation as the value of B_z is scaled indicates the presence of a misaligned B_x or B_y .

the measurements at 1 G and 4 G is $0.1(1.0) \times 10^{-3}$. The misaligned magnetic field that is required to give this change is 9.5 ± 95 mG. If we assume the actual stray field is 100 mG, then the field is a factor of two smaller than the maximum misaligned field we can tolerate. Thus, the error due to a misaligned field is negligible in our measurements.

5.3 Preliminary Data

The final data taken to measure the ratio M_{hf}/β were taken over a period of one week and the conditions of the experiment were changed twice during that period to ensure the measured ratio did not depend on things that we thought it should not, for example collimator angle (which changes the direction of the atomic

beam), alignment of the dye laser into the PBC, and beam density. The raw data with no corrections are shown in Table 5.2. A least squares fit of these data to

Table 5.2: Table of raw data for the ratios $R_I^\pm = (M \pm M_{\text{hf}}/\beta E)(1 + \eta I)$ with no corrections and with $E = 707.63(68)$.

I	$R^+ (10^{-3})$	$R^- (10^{-3})$
2.300	2.5112(06)	1.1602(08)
2.000	2.5047(12)	1.1573(16)
1.500	2.4926(10)	1.1522(24)
1.000	2.4793(29)	—
0.800	2.4775(34)	—

Eq. (5.7) with the correction shown in Eq. (5.6) gives

$$R_I^+ = 2.4636(24) \times 10^{-3}[1 + 0.009522(13)I]. \quad (5.11)$$

The data plotted against this line are shown in Fig. 5.5. The reduced χ^2 for the fit is 0.20 indicating a probability of 90% that the data come from a random distribution.

The correction for photoionization is dominated by the fraction of atoms that make the $E1$ transition. Therefore, the fact that $M_{1_{3 \rightarrow 4}} = M - M_{\text{hf}}$ compared to $M_{1_{4 \rightarrow 3}} = M + M_{\text{hf}}$ has no effect of the correction $(1 + \eta I)$ and we expect that the correction factor η is the same for both ratios. If we use the slope from the R^+ fit to find the least squares fit to the R^- data we find that

$$R_I^- = 1.1357 \times 10^{-3}[1 + 0.009522I]. \quad (5.12)$$

The reduced χ^2 for this fit indicates a 90% probability that the data come from a random distribution. This means the data are consistent with our assumption that both ratios scale the same way with intensity. However, we do not use this fit to determine M_{hf}/β because the poor signal-to-noise ratio on the $F = 4$ to $F' = 3$ transition at low intensities does not allow sufficient precision in the determination

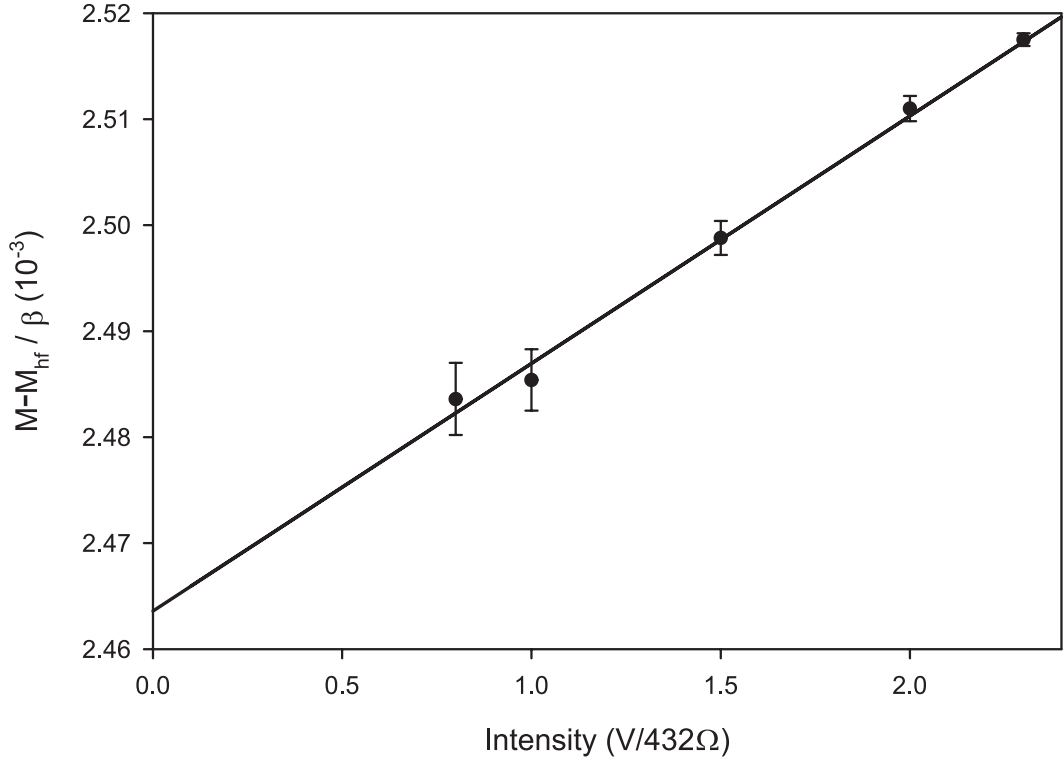


Figure 5.5: Plot of $M - M_{\text{hf}}/\beta$ vs. laser intensity showing the effect of photoionization.

of R_0^- . Instead, we use the ratio R_I^+/R_I^- using data at higher intensities where the signal-to-noise ratio is high. This does allow sufficient precision, and it eliminates the need to determine R_0^- .

The equation

$$\frac{M_{\text{hf}}}{M} = \frac{1 - \sqrt{R_I^+/R_I^-}}{1 + \sqrt{R_I^+/R_I^-}} \quad (5.13)$$

gives the value of M_{hf}/M without the need to make a correction for photoionization effects. The weighted average of R_I^+/R_I^- for the three largest intensities shown in Table 5.2 corrected according to Eq. (5.6) is $R_I^+/R_I^- = 2.1673(14)$. This gives a preliminary value of $M_{\text{hf}}/M = -0.1910(2)$.

The equation

$$\frac{M_{\text{hf}}}{\beta} = \sqrt{R_0^+} \left(1 - \sqrt{\frac{R_I^-}{R_I^+}} \right) \frac{E}{2} \quad (5.14)$$

gives the value of M_{hf}/β . Here it is only necessary to use the determination of R_0^+ , and we can use the more precise values of R^- at higher intensities. The preliminary value is $M_{\text{hf}}/\beta = -5.6325(85)$ V/cm. We can combine this value with $M_{\text{hf}} = -151.86(38) a_0^3$ V/cm [27] to arrive at the value $\beta = 26.962(41)_{\text{expt}} (67)_{\text{theory}} a_0^3$. However, these values need to be corrected for $E2$.

5.4 Accounting for the Electric Quadrupole Amplitude

The data given in the previous section is very nearly the final data, with the effects of magnetic field misalignments, photoionization, offset line centers, asymmetric line shapes, and nonzero background taken into consideration. However, we have not yet considered the effects of the electric quadrupole amplitude ($E2$) in the measurements. If we had a uniform population distribution among the m_F states there would be no correction for the $E2$ amplitude because its effects cancel exactly. (See Appendix B.) We do not have a uniform distribution, as discussed in Section 2.6, so we need to correct the data.

Electromagnetic amplitudes beyond the usual electric and magnetic dipole amplitudes are commonly ignored because of their relatively small size compared to allowed $E1$ and $M1$ amplitudes. However, when dealing with amplitudes such as the PNC $E1$ amplitude and the first-order forbidden $M1$ amplitude, the $E2$ amplitude must be considered to reach accuracies of 0.1%.

Bouchiat and Guéna [27] consider the $E2$ amplitude in their reanalysis of several experiments that determine the ratio M_{hf}/M for the $6S \rightarrow 7S$ transition in cesium. In particular, they say that the work of Ref. [28] does not measure M_{hf}/M ,

but instead measures the ratio

$$R = \frac{M_{\text{hf}}}{M} \left(1 - \frac{3}{4} \frac{E2}{M_{\text{hf}}} \right). \quad (5.15)$$

Clearly, if the ratio $E2/M_{\text{hf}}$ is small enough, there is no error. However, the results of Ref. [27] indicate that $E2/M_{\text{hf}} = 42(13) \times 10^{-3}$ and so $M_{\text{hf}}/M = -0.1886(17)$ rather than the value $M_{\text{hf}}/M = -0.1830(4)$ found in Ref. [28]. Indeed, if we compare this with our result of $M_{\text{hf}}/M = -0.1910(2)$, there is clearly a discrepancy.

As shown in Appendix B, if we have the population distributions calculated by Peter Marte, then the measurements of the ratio R^+ need a -0.094% correction and the measurements of the ratio R^- need a $+0.079\%$ correction. This is a small but significant correction to our data. The revised numbers that follow assume that there is a 50% uncertainty in these corrections, mainly from the uncertainty in the determination of the population distribution.

To arrive at the fractional corrections in the previous paragraph, we begin by assuming that the $E2$ amplitude does not affect our measurements. The difference between the values of M_{hf}/M determined by the present experiment and in Ref. [28] then gives us the value of $E2/M_{\text{hf}}$ using the equation

$$\left(\frac{M_{\text{hf}}}{M} \right)_{\text{present}} = \left(\frac{M_{\text{hf}}}{M} \right)_{\text{Ref. [28]}} \left(1 - \frac{3}{4} \frac{E2}{M_{\text{hf}}} \right)^{-1}. \quad (5.16)$$

Then we use this value of $E2/M_{\text{hf}}$ to correct our data for the $E2$ contributions. Our new value of M_{hf}/M can again be compared with that of Ref. [28] to determine an improved value of $E2/M_{\text{hf}}$, and so on. This procedure is iterated until we arrive at an internally consistent value of $E2/M_{\text{hf}}$. Our final value is $E2/M_{\text{hf}} = 53(2) \times 10^{-3}$, which gives the corrections mentioned above. The final results for this experiment are given in Table 5.3. Our new value of β is compared to previous results in Fig. 5.6.

Table 5.3: Final results for the M_{hf}/β experiment. The uncertainties shown are one sigma values. In the first three values, the uncertainty is purely experimental, and in the final value the uncertainties have been separated into their contributions from experiment and theory.

Quantity	Without $E2$ Correction	With $E2$ Correction
$E2/M_{\text{hf}}$	–	0.053(3)
M_{hf}/M	–0.1910(2)	–0.1906(3)
M_{hf}/β (V/cm)	–5.6325(85)	–5.6195(91)
β (a_0^3)	26.962(41) _{expt} (67) _{theory}	27.024(43) _{expt} (67) _{theory}

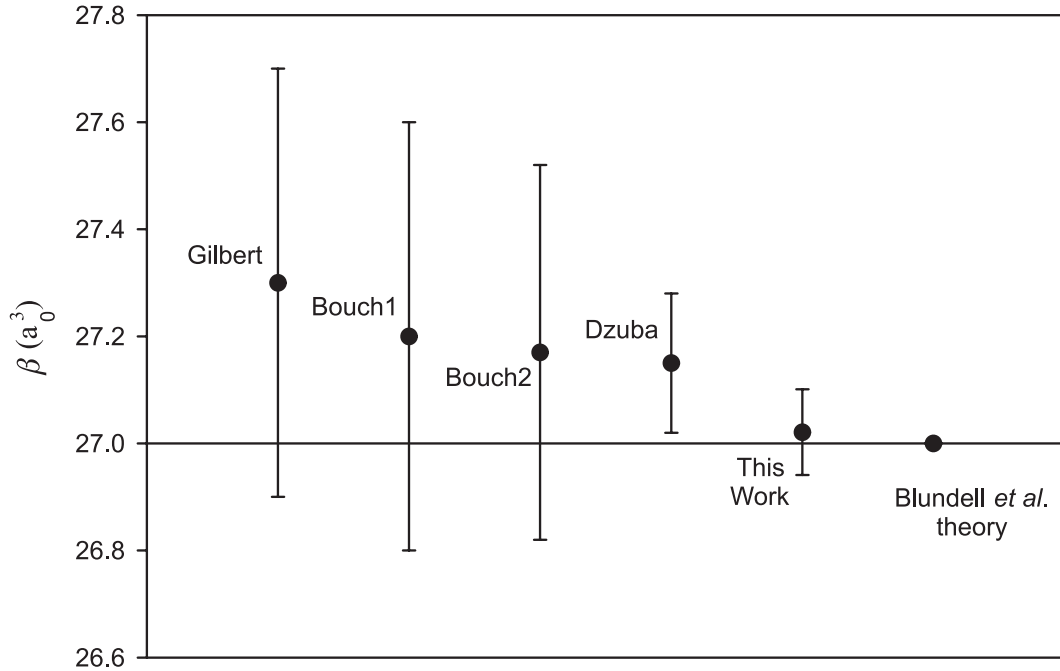


Figure 5.6: An historical comparison of the determinations of β . Gilbert is from Ref. [57], Bouch1 is from Ref. [58], Bouch2 is from Ref. [59], Dzuba is from Ref. [24], and the theory is from Ref. [14].